



Article

---

# Assessment of Morphometric Parameters as the Basis for Hydrological Inferences in Water Resource Management: A Case Study from the Sinú River Basin in Colombia

---

Alvaro López-Ramos, Juan Pablo Medrano-Barboza, Luisa Martínez-Acosta, Guillermo J. Acuña, John Freddy Remolina López and Alvaro Alberto López-Lambraño

Special Issue

Geo-Information for Watershed Processes

Edited by

Prof. Dr. Walter Chen and Prof. Dr. Fuan Tsai



Article

# Assessment of Morphometric Parameters as the Basis for Hydrological Inferences in Water Resource Management: A Case Study from the Sinú River Basin in Colombia

Alvaro López-Ramos <sup>1</sup>, Juan Pablo Medrano-Barboza <sup>1</sup> , Luisa Martínez-Acosta <sup>1</sup> , Guillermo J. Acuña <sup>2</sup> ,  
John Freddy Remolina López <sup>3</sup>  and Alvaro Alberto López-Lambrano <sup>4,5,6,\*</sup> 

<sup>1</sup> GICA Group, Department of Civil Engineering, Universidad Pontificia Bolivariana Campus Montería, Carrera 6 # 97A-99, Montería 230002, Córdoba, Colombia

<sup>2</sup> CAMHA Group, Department of Sanitary and Environmental Engineering, Universidad Pontificia Bolivariana Campus Montería, Carrera 6 # 97A-99, Montería 230002, Córdoba, Colombia

<sup>3</sup> ITEM Group, Department of Electronic Engineering, Universidad Pontificia Bolivariana Campus Montería, Carrera 6 # 97A-99, Montería 230002, Córdoba, Colombia

<sup>4</sup> Faculty of Engineering, Architecture and Design, Universidad Autónoma de Baja California, Mexicali 22860, Mexico

<sup>5</sup> Hidrus S.A. de C.V., Ensenada 22760, Mexico

<sup>6</sup> Grupo Hidrus S.A.S., Montería 230002, Córdoba, Colombia

\* Correspondence: alopezl@uabc.edu.mx; Tel.: +521-442-194-6654 or +521-646-134-5766



**Citation:** López-Ramos, A.; Medrano-Barboza, J.P.; Martínez-Acosta, L.; Acuña, G.J.; Remolina López, J.F.; López-Lambrano, A.A. Assessment of Morphometric Parameters as the Basis for Hydrological Inferences in Water Resource Management: A Case Study from the Sinú River Basin in Colombia. *ISPRS Int. J. Geo-Inf.* **2022**, *11*, 459. <https://doi.org/10.3390/ijgi11090459>

Academic Editors: Walter Chen, Fuan Tsai and Wolfgang Kainz

Received: 9 July 2022

Accepted: 18 August 2022

Published: 24 August 2022

**Publisher's Note:** MDPI stays neutral with regard to jurisdictional claims in published maps and institutional affiliations.



**Copyright:** © 2022 by the authors. Licensee MDPI, Basel, Switzerland. This article is an open access article distributed under the terms and conditions of the Creative Commons Attribution (CC BY) license (<https://creativecommons.org/licenses/by/4.0/>).

**Abstract:** The geomorphology of a basin makes it possible for us to understand its hydrological pattern. Accordingly, satellite-based remote sensing and geo-information technologies have proven to be effective tools in the morphology analysis at the basin level. Consequently, this present study carried out a morphological analysis of the Sinú river basin, analyzing its geometric characteristics, drainage networks, and relief to develop integrated water resource management. The analyzed zone comprises an area of 13,971.7 km<sup>2</sup> with three sub-basins, the upper, the middle, and the lower Sinú sub-basins, where seventeen morphometric parameters were evaluated using remote sensing (RS) and geographical information system (GIS) tools to identify the rainwater harvesting potential index. The Sinú basin has a dendritic drainage pattern, and the results of the drainage network parameters make it possible for us to infer that the middle and lower Sinú areas are the ones mainly affected by floods. The basin geometry parameters indicate an elongated shape, implying a lesser probability of uniform and homogeneous rainfall. Additionally, the hypsometric curve shape indicates that active fluvial and alluvial sedimentary processes are present, allowing us to conclude that much of the material has been eroded and deposited in the basin's lower zones as it could be confirmed with the geological information available. The obtained results and GIS tools confirm the basin's geological heterogeneity. Furthermore, they were used to delimit the potential water harvesting zones following the rainwater harvesting potential index (RWHPI) methodology. The research demonstrates that drainage morphometry has a substantial impact on understanding landform processes, soil characteristics, and erosional characteristics. Additionally, the results help us understand the relationship between hydrological variables and geomorphological parameters as guidance and/or decision-making instruments for the competent authorities to establish actions for the sustainable development of the basin, flood control, water supply planning, water budgeting, and disaster mitigation within the Sinú river basin.

**Keywords:** watershed management; watershed land surface; geo-information technology; morphology; relief

## 1. Introduction

A hydrographic basin is an area partly or entirely drained by several watercourses and delimited by an imaginary line formed by points of the highest topographic elevation

called watershed, which separates it from neighboring basins [1]. To this extent, just as the hydrological cycle is the fundamental concept in hydrology, the hydrographic basin is a naturally defined hydrological unit that becomes the basis for any study of water resource management [2]. In a basin, morphometry makes it possible to quantitatively study, from a mathematical point of view, the surface configuration as well as the shape and relief [3]. Horton [4] proposed the bases for the quantitative description of a hydrographic basin's shape and drainage network in addition to the interrelationships between morphometry, climate, vegetation, and soil properties. Similarly, it has been established that given the unidirectional water flow, processes in the upper parts of the basin invariably have repercussions in the lower part and the basin morphometric characteristics have a decisive influence on its hydrological response [5]. It is also paramount to note that through morphometry study, it is possible to describe and even predict flow behavior corresponding to the water courses that drain it, and thus, quantify the surface and underground water potential, making it possible to analyze alternatives to the use of water resources in areas where it is required [6,7].

Contrastingly, the hydrological response of a basin and its geological history can be described from morphometric parameters such as area, altitude, slope, shape, drainage density, and length of streams by correlating them with hydrological phenomena such as runoff [8]. In other words, the basin response to a series of precipitation events depends, on one hand, on the rain properties (intensity, duration, frequency, and so on) and, on the other, on the basin's morphological and geological features.

Therefore, morphometric characterization is significant in hydrological research and in studies regarding the management and conservation of natural resources. Such is the case of the Adnan et al. [9] research, which estimated the morphometric parameters of the Karnaphuli and Sangu basins in Bangladesh to assess the region's susceptibility to flash flood events and obtain a flood risk map for the area.

In the case of Gajbhiye et al., Malik et al., Nitheshnirmal et al., and Rahmati [10–13], they determined the morphometric parameters in different drainage basins to assess the susceptibility to erosion and concluded that it was necessary to establish effective practices for land use and water resource management in these basins. In a similar manner, using geographic information systems and the morphometric characteristics of a basin, potential rainwater harvesting (RWH) zones can be determined through multi-criteria decision analysis, which involves establishing suitability criteria and Boolean logic [14,15]. Regarding the study of the rain-runoff phenomenon in hydrographic basins, Jena and Tiwari [16] performed a correlation analysis between morphometric parameters and the features of the unit hydrographs of the Tarafeni and Bhairabanki basins in India, thus obtaining nonlinear regression models to generate synthetic unit hydrographs.

Meanwhile, Viramontes-Olivas et al. [17] analyzed the morphometric parameters of the San Pedro Chonchos river basin in Chihuahua, Mexico, noticing that drainage density is influenced by vegetation cover and lithology, since it regulates infiltration rates and feeding of the subsurface flow, thus reducing the effects and impact of possible floods in the basin.

The geomorphological features of a basin can also be used to determine the homogeneous regions in which hydrological response to a precipitation event is similar. In that aspect, from the correlation of these features with the hydrological variables, it becomes possible to transfer hydrological information in sites with missing or incomplete data [18]. Hence, based on the methods proposed by Horton [4,19], Schumm [20], Strahler [21], and Shreve [22], the characterization of multiple basins has been successfully achieved to obtain reliable information on the hydrological response and physical characteristics of the soil, such as permeability and even from the present parent rock.

Nonetheless, these methods are usually complex and time-consuming (weeks, even months) when used to analyze large areas, especially when there are basins that can exceed 1000 km<sup>2</sup> [23]. As a result, in recent years, hydrological research has been supported through geographic information systems (GIS) since it is a technique specialized in handling large data sets, allowing time optimization for its analysis and understanding of the

spatial distribution of the variables to analyze. This represents an improvement in the systematization of the description, comparison, and classification of hydrographic basins regardless of their extension, this being of great use and applicability in hydrology [24–29].

Consequently, this study aims to: (1) determine the morphometric parameters of the Sinú river basin in Colombia through GIS and existing cartography to characterize its drainage network and morphology; (2) analyze the morphometric parameters relationship with erosion and floods in the Sinú river basin; and (3) based on the obtained results, determine the areas with rainwater harvesting potential within the basin as an alternative to mitigate floods and drought situations in the study area. Moreover, considering the lack of hydrological information in the basin, these analyses provide valuable information to improve hydrological models and to integrally manage the basin's water resources, since these results can be the foundations for decision-making standards and guidelines focused on sustainable development, natural resource conservation, land use planning and management, flood risk mitigation, and water supply for the communities of the study area.

## 2. Area of Study

The Sinú river basin is located in the northwestern part of Colombia, between 9°30' N to 7°05' N and 76°35' W to 75°15' W. It has an area of 13,972 km<sup>2</sup>, in the jurisdiction of the departments of Córdoba, Sucre, and Antioquia, and according to the provisions of the Regional Autonomous Corporation of the Sinú and San Jorge Valleys, CVS (for its acronym in Spanish), it is divided in accordance with its geographical and biotic characteristics in three zones: the upper, middle and lower Sinú zones or regions, CVS [30].

The geographical location, municipalities, and departments in which the Sinú river basin is located can be seen in Figure 1. Mainly, the basin consists of elevations below 300 masl in the lower and middle Sinú region, while in the upper Sinú region there are heights higher than 1000 masl. The Sinú river has its source in this area, specifically in the Nudo del Paramillo at an altitude of 3400 masl, crossing the basin from south to north until reaching its mouth at the Caribbean Sea in Boca de Tinajones through three mouths called Mireya, Medio, and Corea, in the municipality of San Bernardo del Viento, CVS [30].

Conversely, the main population centers of the basin are: Tierralta and Valencia in the upper basin, Montería (capital of the Córdoba department) in the middle, and Loricá in the lower basin. Furthermore, in the upper basin there is also the URRÁ hydroelectric plant and the Paramillo National Natural Park [31].

According to the Agustín Codazzi Geographical Institute, IGAC (for its acronym in Spanish) [32], there are different types of landscapes in the basin distributed within the two large geo-structures, where the region's great geomorphological diversity is evident. In the mountain range (Cordillera), landscapes of high hills and ridges represent 19.72% of the area, while in the sedimentation mega basin, the greatest diversity of landscapes are found, with a predominance of lowland landscape, occupying 70.02% of the basin, and the hillside, 7.99% of the territory.

Figure 2 presents the map of the chronostratigraphic units (CSU) and geological faults of the study area, identified by bearing in mind the International Chronostratigraphic Chart [33], corresponding to a code formed by the geochronological age notation separated with a hyphen of an acronym that indicates the rock type and its formation environment (V: volcanic, H: hypabyssal, P: plutonic, VC: volcanoclastic, S: sedimentary, and M: metamorphic) followed by a lower case letter representing its composition, metamorphism grade, or accumulation environment depending on whether igneous, metamorphic, or sedimentary rocks are involved, respectively, e.g., u: ultramafic, lg: low grade of metamorphism, ct: continental-transitional [34]. In the case of the study area, it is evident that UC Q-al, e3e4-Sm, and n6n7-Sm prevail, corresponding, respectively to alluvial and alluvial plain deposits, grainy-decreasing conglomeratic lithic arenites and intercalations of mudstones, and calcareous arenites and coarse-grained to conglomeratic quartz sandstones.

It is estimated that the 2010–2011 flood event affected 178,124 people in the Sinú River basin, representing 18% of the population of the affected municipalities, and 30,257 houses, representing 15.9% of the households. In addition, it is estimated that 50–60% of this population was in a critical condition, with percentage of unmet basic needs (UBN) values of 40%, suggesting that the greatest impacts were received by municipalities with highly deficient structural conditions [35].

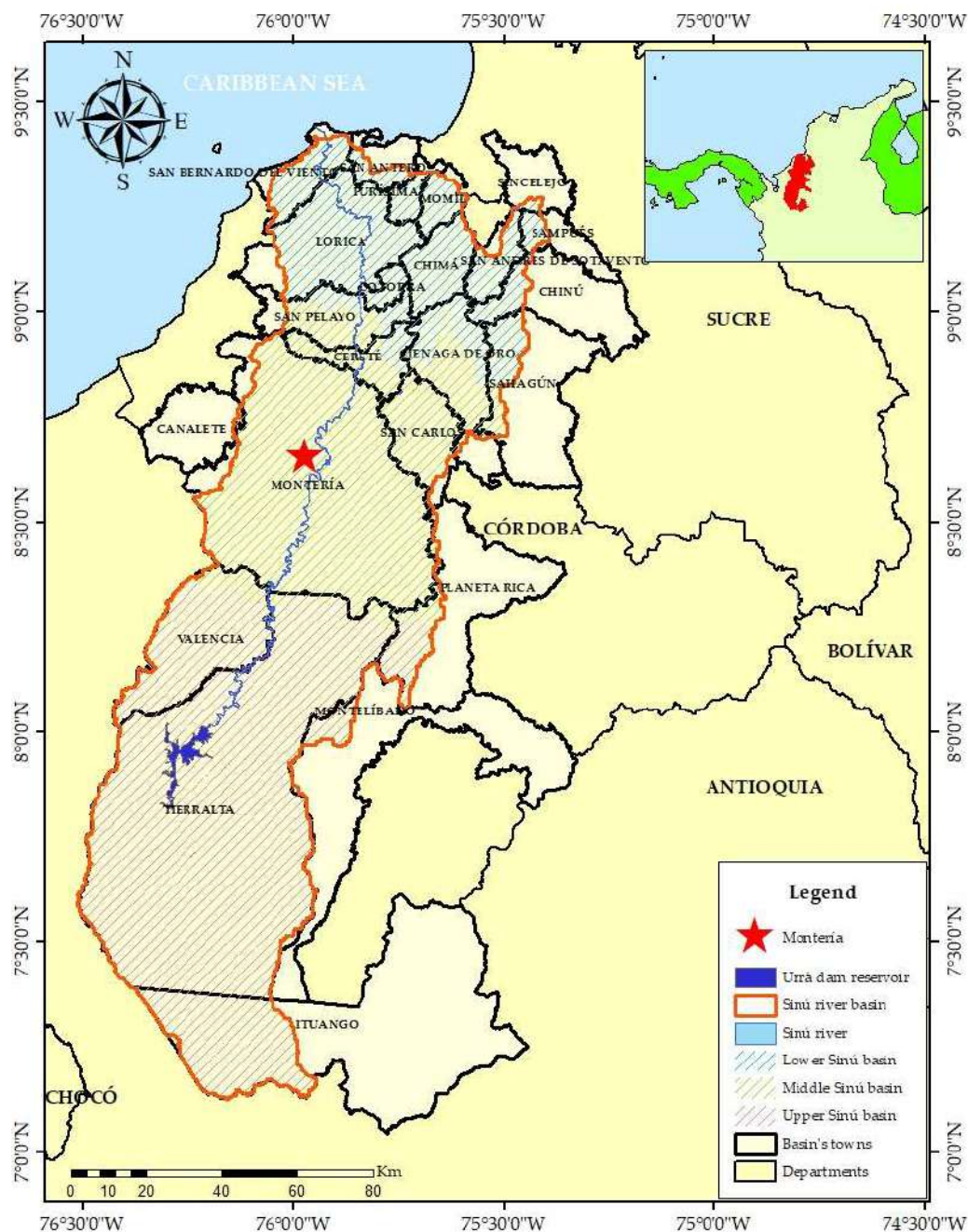


**Figure 1.** Location of the Sinú river basin in Colombia. The map shows the position of Montería city as the most representative urban area, the Sinú river, and the Urrá hydroelectric dam.

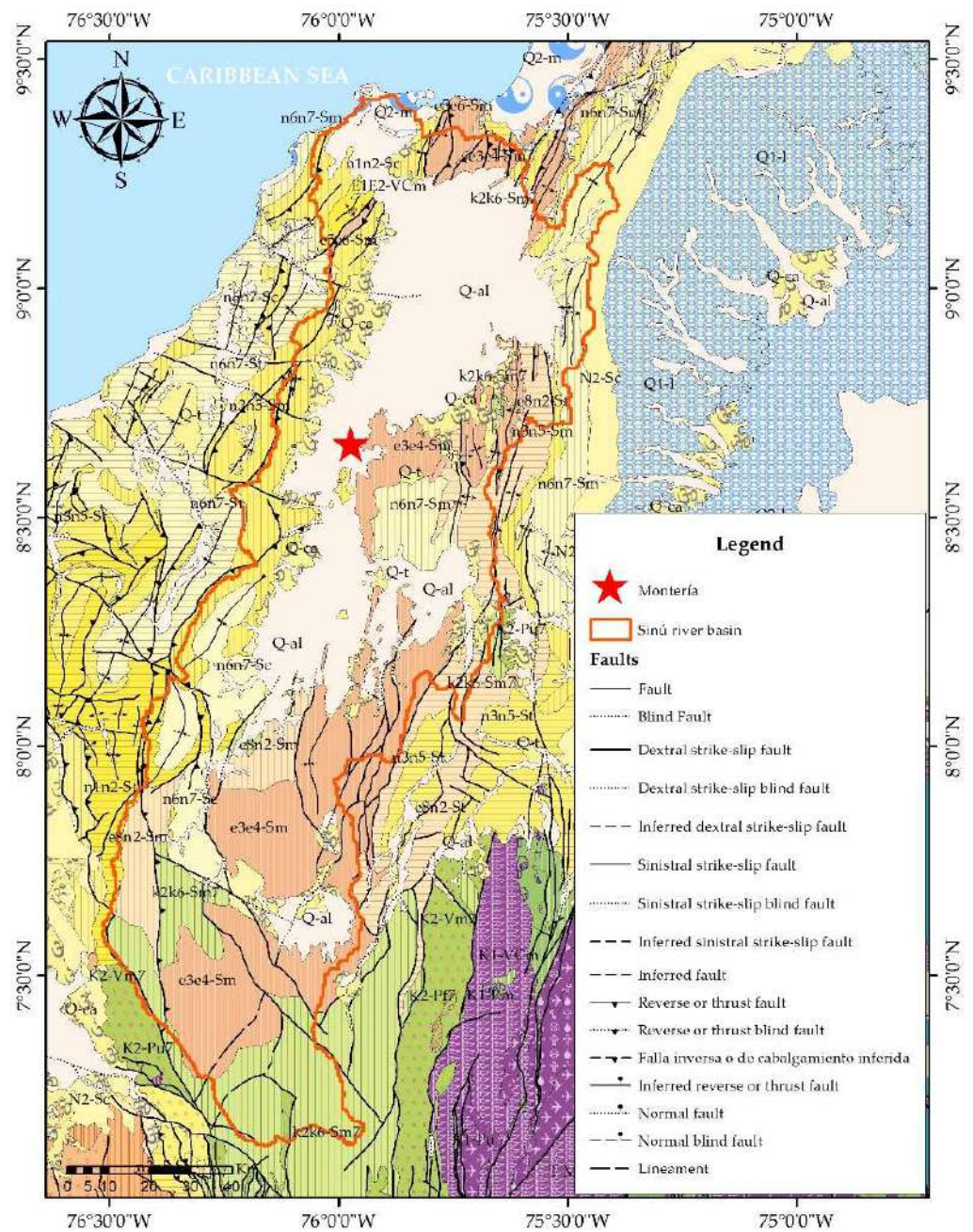


Figure 2. Chronostratigraphic units (CSU) and geological faults of the study area.

This impact caused by floods in the Sinú basin is closely linked to the development of activities in potentially floodable zones (PFZ). The National Water Study prepared by the Institute of Hydrology, Meteorology, and Environmental Studies, IDEAM (for its acronym in Spanish) [36] estimated that for the Sinú basin, about 76% of the PFZ has been transformed into agricultural territories or artificial zones. According to information from CVS [37], the points identified by drainage erosion problems and those present threats due to flooding on the Sinú river are located in the municipalities of Tierralta and Valencia in the upper Sinú sub-basin; Montería, Cereté, and San Pelayo in the middle Sinú, and Cotorra, Lorica, and San Bernardo del Viento in the lower Sinú sub-basin, occurring mostly in Lorica (24%), Tierralta (22%), and Montería (21%). The largest number of people who have been affected due to flood events are in the San Pelayo Municipality, followed by the Lorica and Cotorra municipalities. Regarding economic affectations, they are related to the productive and agro-industrial system and the most affected municipalities are: San

Pelayo, San Bernardo del Viento, and Tierralta. Finally, in terms of territorial effects, the municipalities in the basin with the largest number of flooded hectares are usually Cotorra and Loricá.

### 3. Materials and Methods

For the morphometric analysis of the basin through GIS, the use of a digital elevation model (DEM) was required, which, according to Felicísimo [38], is a numerical data structure that represents the spatial distribution of altitude on the earth's surface, i.e., it is a set of matrices resulting from superimposing a grid on the terrain and extracting the average altitude of each cell, so they are a regular square mesh network with equally spaced rows and columns. To delimit the watershed, different elevation models were used: SRTM from the Shuttle Radar Topographic Mission with 30-m resolution, the ALOS PALSAR RTC with 12.5 m resolution, and the Hydroshed Digital Elevation Model developed by the United States Geological Survey—USGS, which was validated by the Inter-American Development Bank (IDB) in the framework of the Integrated Model of Climate Change and Water Resources with a 460 m × 460 m resolution [39,40].

To evaluate the accuracy of the DEM, the generation of stream definition was performed using several thresholds, and the result was compared with the official cartographic plates, determining that, since most of the study area is characterized by being flat and with little slope, there was a considerable difference between the real drainage network and the one obtained using the GIS tools, especially when generating the main stream, the Sinú river in this case. Additionally, control points were taken in order to estimate the mean squared error (MSE) of the elevations, concluding that the DEMs had MSEs in the order of 5 to 20 m in some sectors, especially in the middle and lower basin of the Sinú river. Finally, it was found that none of the digital elevation models (DEMs) satisfactorily represented the drainage network; however, although the HydroSHED Digital Elevation Model was the one that best represented the basin polygon, no significant differences were found regarding the other analyzed models, the reason for which it was decided to use the ALOS PALSAR RTC DEM to delineate the basin and use the digitized drainage network of the cartographic plates to estimate the basin morphometric parameters. This DEM made it possible to know the spatial distribution of the terrain elevations in the study area and, from this, estimate slopes and other relief aspects. In this manner, with the GIS, it was possible to determine the directions of flow, the delimitation of sub-basins, and the schematization of streams that drain it from a threshold.

The methodology used to obtain the drainage network of the Sinú river basin is shown in Figure 3, where the input parameters are shown in blue, the procedures carried out on the information in yellow, and the files names generated at each step in green. Thus, through GIS, a filling of the sinks was carried out to correct errors that could occur due to the data resolution or the rounding of elevations to the nearest integer value, and, once a DEM without sinks was obtained, the flow direction from the differences in elevation and slope was determined [41]. Later, to outline the water courses that drain the Sinú river basin, flow accumulation was estimated, which is just the number of cells on the slope that flow towards each cell, and thus the streams were defined.

Afterwards, the order of the streams was established with the Horton classification system [4] to subsequently generate the polygons of the sub-basins and make manual corrections to calibrate the model, obtaining a total of 65 sub-basins: 6 corresponding to the lower Sinú, 18 to the middle Sinú, and the remaining 41 to the upper Sinú region (Figure 4).

With the information generated from the terrain modeling, the morphometric parameters were estimated from the methods and formulas proposed by Horton [4,19], Schumm [20], Strahler [21], and Mueller [42] (Table 1). Results were also used to determine the potential rainwater harvesting areas using GIS-based multi-criteria decision analysis [14,43]. Finally, the existing cartography for the area was consulted to compare and validate the results of the morphometric parameters of the drainage network, such as drainage density and channel frequency, with those obtained from the modeling data, given

that these parameters are sensitive to scale and, thus, results of the parameters estimated from the analysis with a threshold of 25 km<sup>2</sup> would not be the same as those estimated when using the 1:25,000 scale cartographic plates from the IGAC [44].

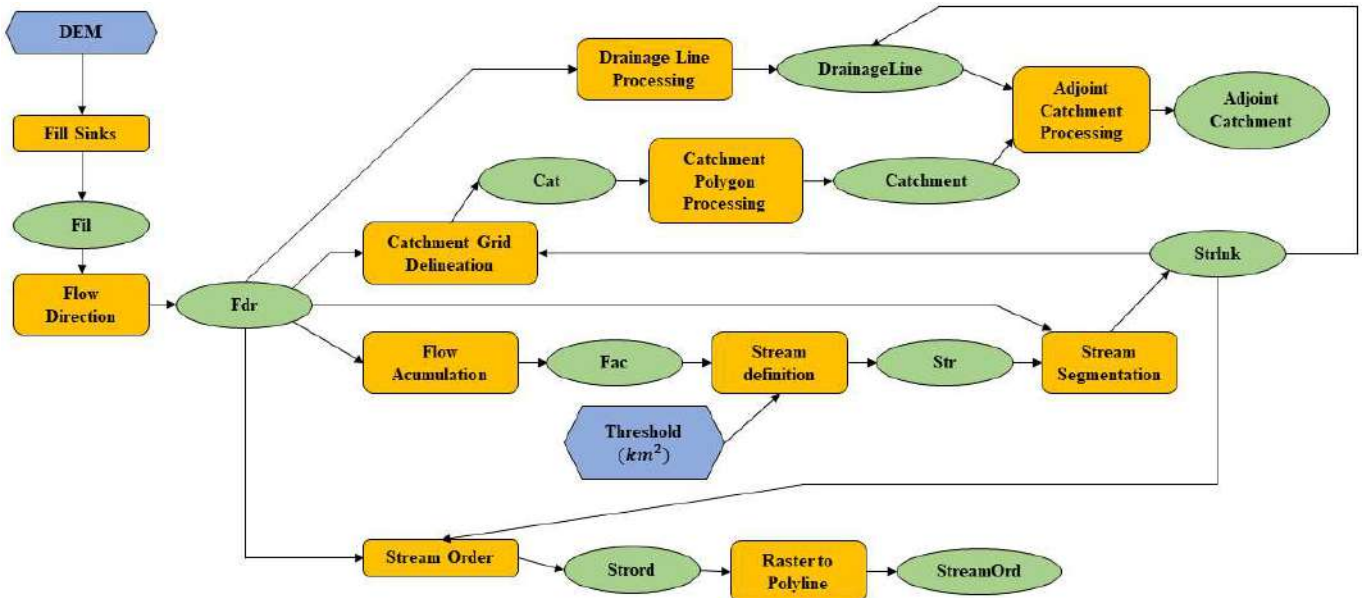


Figure 3. Flowchart of the methodology for watershed characterization through GIS.

The morphometric parameters calculated can be defined as follows:

Table 1. Morphometric Parameters used in the Study.

| Morphometric Parameter                    | Formula/Definition  | Reference |
|---|---|-----------|
| <b>Drainage network</b>                   |   |           |
| Stream order                              | Hierarchical rank.  | [4,21]    |
| Stream length ( $L$ )                     | Main channel length of the stream (km)  | [4]       |
| Stream length ( $L_u$ )                   | Total stream length (km)/GIS software analysis  | [4]       |
| Number of streams ( $N_u$ )               | Total stream number of a given order/GIS software analysis                                    | [4]       |
| Stream axial length ( $L_a$ )             | Shortest distance between the beginning and the outlet of a stream (km)/GIS software analysis | [42]      |
| Drainage density ( $D_d$ )                | $D_d = \frac{L}{A_d}$ , km/km <sup>2</sup>  | [4]       |
| Length of overland flow ( $L_{OF}$ )      | $L_{ft} = \frac{1}{2D_d}$ , km  | [4]       |
| Constant of channel maintenance ( $C_m$ ) | $C_m = \frac{1}{D_d}$ , $\frac{\text{km}^2}{\text{km}}$                                       | [20]      |
| Stream frequency ( $F$ )                  | $F = \frac{N}{A_d}$ , streams/km <sup>2</sup>   | [4]       |
| Average stream length ( $L_m$ )           | $L_m = \frac{L_u}{N_u}$   | [4]       |
| Sinuosity ( $S$ )                         | $S = \frac{L}{L_u}$   | [42]      |
| Bifurcation ratio ( $R_b$ )               | $R_b = \frac{N_u}{N_{u+1}}$   | [4]       |
| Mean bifurcation ratio ( $R_{bm}$ )       | $R_{bm} = \frac{\sum(R_{bu}/R_{bu+1})(N_u + N_{u+1})}{\sum(N_u + N_{u+1})}$                   | [20]      |
| Stream length ratio ( $R_l$ )             | $R_l = \frac{L_u}{L_{u-1}}$   | [4]       |
| <b>Basin geometry</b>                     |   |           |
| Basin area ( $A_d$ )                      | Plan area of the watershed (km <sup>2</sup> )   | [4]       |
| Basin perimeter ( $P$ )                   | GIS software analysis (km)  | [4]       |
| Basin length ( $L_c$ )                    | Maximum basin length (km)/GIS software analysis.  | [19]      |
| Form factor ( $F_f$ )                     | $F_f = \frac{A_d}{L_c^2}$   | [19]      |
| Circularity ratio ( $R_c$ )               | $R_c = \frac{A_d}{\frac{P^2}{4\pi}}$  | [45]      |



Table 1. Cont.

| Morphometric Parameter             | Formula/Definition                    | Reference |
|------------------------------------|---------------------------------------|-----------|
| Elongation ratio ( $R_e$ )         | $R_e = \frac{D_c}{L_c}$               | [20]      |
| Compactness coefficient ( $K_c$ )  | $K_c = \frac{L_c^2}{2\sqrt{\pi A_d}}$ | [19]      |
| <b>Basin relief</b>                |                                       |           |
| Minimum basin height ( $H_{min}$ ) | GIS software analysis (masl).         | [20]      |
| Maximum basin height ( $H_{max}$ ) | GIS software analysis (masl).         | [20]      |
| Mean basin slope ( $S_c$ )         | GIS software analysis (%).            | [20]      |
| Basin relief ( $H$ )               | $H = H_{max} - H_{min}$               | [20]      |
| Relief ratio ( $F_H$ )             | $F_H = \frac{H}{L_c}$                 | [20]      |

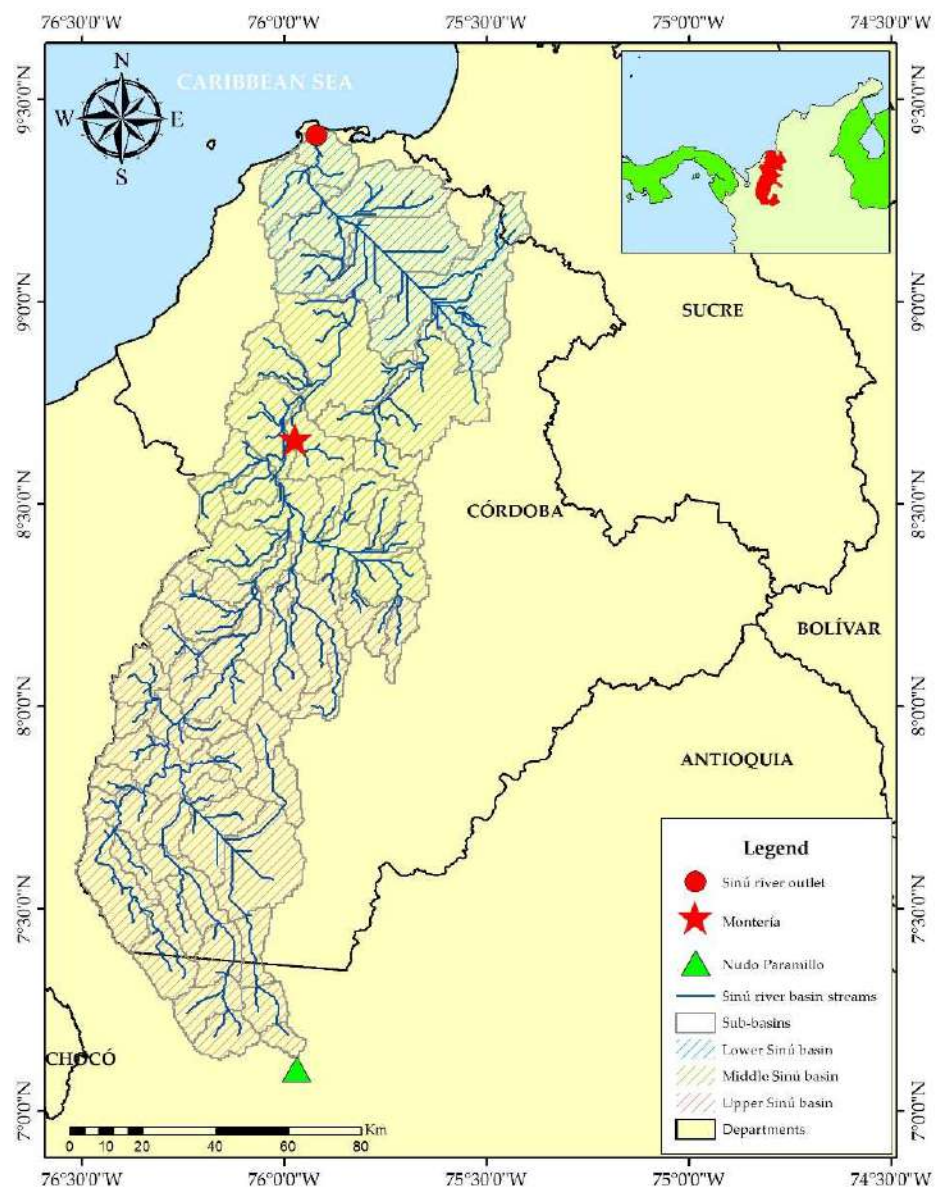


Figure 4. Characterization of the Sinú river basin in Colombia through GIS. The drainage network of the basin and the 65 sub-basins obtained are shown.

### 3.1. Stream Order

The stream order makes it possible to explain the hydrological behavior of a basin, since it is directly proportional to the area, the cross section of the course, and the flow that

it transports. This way, it is expected that the channels of higher order drain larger areas and, thus, transport a much higher flow [6,46].

### 3.2. Number of Channels of Order $u$ ( $N_u$ )

According to the stream number law established by Horton [4], “the number of streams of different orders in any basin tends to be estimated as inverse geometric series, of which the first term is unity and the ratio is the bifurcation ratio”.

### 3.3. Length of Channels of Order $u$ ( $L_u$ )

Length of channels of order  $u$  is calculated by measuring the length of all streams of a given order within the catchment [4].

### 3.4. Drainage Density ( $D_d$ )

Drainage density corresponds to the total length of streams per unit area and makes quantitative determination of whether a basin is well or poorly drained possible [4]. This parameter is related (together with the number of channels of order  $u$ ) to aspects such as soil erosion and runoff, since the flow is directly proportional to the drainage density, which translates into rapid runoff that implies an increase in the peak flow of the hydrograph. Additionally, drainage density has an inverse relationship with infiltration, since high infiltration tends to inhibit the development of longer drainages, i.e., the lowest drainage densities correspond to regions with permeable soil types, dense vegetation, and low relief, while the high drainage density prevails in regions with impermeable soils, sparse vegetation, and high relief [10,21,47].

### 3.5. Overland Flow Length ( $L_{OF}$ )

Horton [4] defined the length of the overland flow as the distance that the water must travel on the ground surface before reaching the channels of the drainage network, and also estimated that it is approximately equal to half the reciprocal of the density drainage.

### 3.6. Constant of Channel Maintenance ( $C_m$ )

This parameter corresponds to the inverse of the drainage density and makes it possible to estimate the amount of area in  $\text{km}^2$  necessary for the maintenance of 1 km of channel [20,48].

### 3.7. Stream Frequency ( $F$ )

Stream frequency was defined by Horton [4] as the number of stream channels per unit area.

### 3.8. Sinuosity of Currents ( $S$ )

Considering that all watercourses must adjust to the terrain irregularities along their route, Mueller [42] proposed sinuosity as an index that allows these variations in the course of the channel to be measured from the ratio between the stream total length (km) and the shortest distance between its beginning and mouth (km).

### 3.9. Bifurcation Ratio ( $R_b$ )

The bifurcation ratio is the ratio of the number of channels of a specific order and the number of streams of the next order [4]. It is a parameter that reflects both the complexity of the ramifications in the basin and its geometric shape, and it is also related to factors such as slope and area physiography.

### 3.10. Length Ratio ( $R_l$ )

According to Horton’s research [4], length ratio is the result of dividing average length of the flow of any order by average length of the next lower order.

### 3.11. Form Factor ( $F_f$ )

The shape factor of the basin is a parameter that makes it possible to know the geometry of the basin and is also related to the flows of the drainage network [19].

### 3.12. Circular Ratio ( $R_c$ )

Miller [45] defines this parameter as the ratio between area of the basin and area of a circle that has the same circumference as the basin perimeter and in this manner, if it takes values close to the unit, it indicates that the shape of the basin resembles a circle.

### 3.13. Elongation Ratio ( $R_e$ )

The elongation ratio corresponds to the ratio between the diameter of a circle with the same basin area ( $D_c$ ) and the maximum basin length ( $L_c$ ), and like  $R_c$ , it has a maximum value of one for perfectly round basins [20]. The  $R_e$  generally varies from 0.6 to 1.0 and depends on climate and the geology of the study area. Furthermore, these values can be grouped into: circular for  $R_e > 0.9$ , oval for  $0.9 > R_e > 0.8$ , and less elongated when  $R_e < 0.7$  [49].

### 3.14. Compactness Coefficient ( $K_c$ )

According to Horton's research [19], compactness coefficient is the relationship between the basin's perimeter and a circle with the same area, thus, the closer the result is to the unit, the more circular the basin will be.

### 3.15. Mean Slope of the Basin ( $S_c$ )

The study of slope distribution is important because it provides data for activities such as planning of engineering works, reforestation, mechanization of agriculture, and others [50]. Additionally, it makes the evaluation of the volumes and direction of surface runoff possible [51].

### 3.16. Relief Factor ( $F_H$ )

The basin relief features play an important role in the development of the drainage network, superficial flow, permeability, and susceptibility to soil erosion. The basin relief ( $H$ ) is then defined as the difference between maximum and minimum height.

### 3.17. Hypsometric Curve of the Basin

The hypsometric curve is the graphic representation of the basin relief, where its ordinate represents elevation in meters above sea level, and its abscissa, the area in  $\text{km}^2$  that is between two levels.

### 3.18. Rainwater Harvesting Potential Index (RWHPI)

According to the conducted literature review, rainwater harvesting (RWH) is one of the most usual practices as an alternative to mitigate water scarcity and other environmental problems; moreover, as stated by Singh et al. [14], the planning and implementation of water harvesting projects is a multi-criteria and multi-objective problem because it depends on several factors.

In order to identify sites where the implementation of water harvesting techniques is viable, GIS tools were used to delimit the potential water harvesting zones following the methodology of rainwater harvesting potential index (RWHPI) proposed by Singh et al. [14]. Thus, the runoff coefficient, slope, and drainage density layers were used.

## 4. Results

### 4.1. Drainage Network

The DEM was used to determine the basin relief analysis including the hypsometric curve and slope calculation. From the information mentioned, it was found that the

maximum order of the basin is 5, corresponding in this case to the courses of 4 and 5 order for the Sinú river (Figure 5).

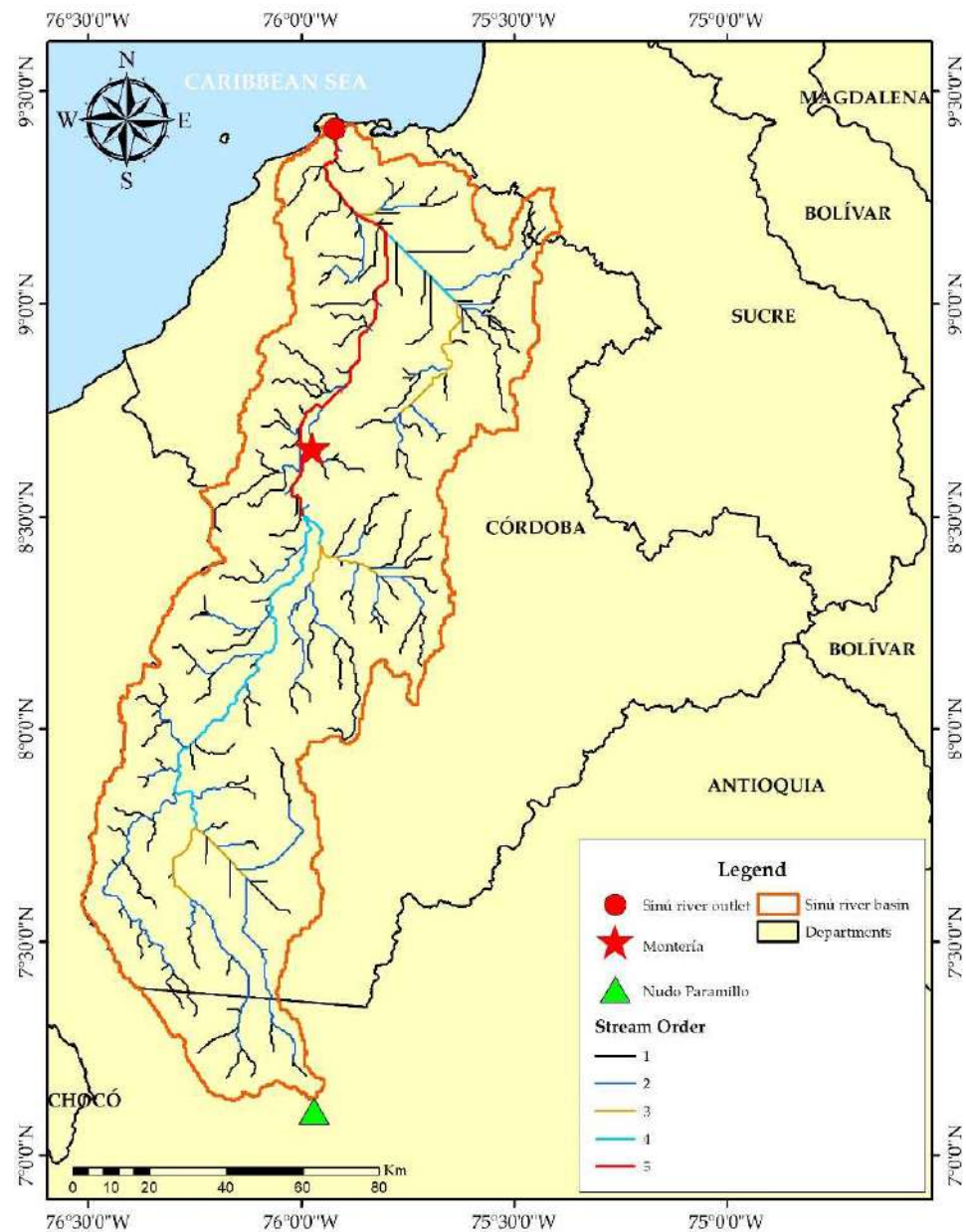


**Figure 5.** Stream order of the drainage network of the Sinú river basin (Colombia), schematized by GIS.

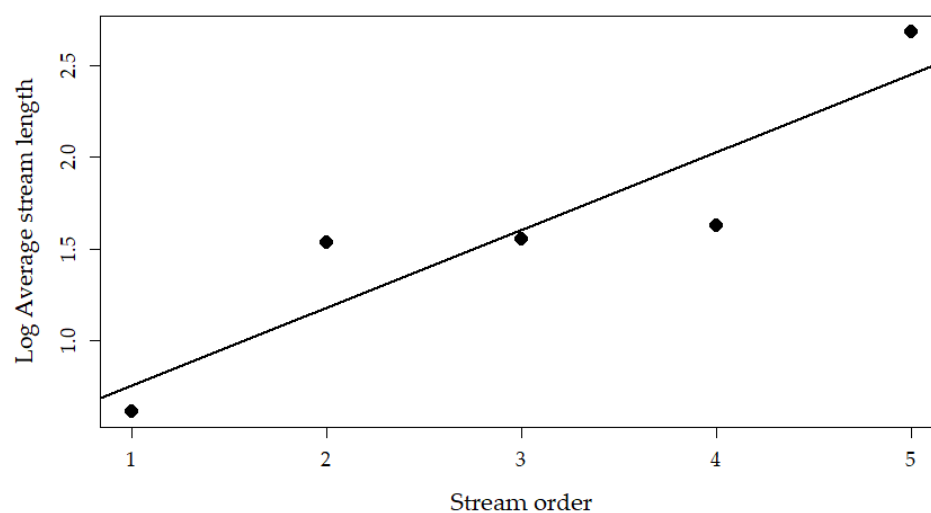
In the analysis, the Sinú river basin shows an order of 5 value with a dendritic drainage pattern, characterized by having a tree-like distribution with tributary branches in many directions and with variable angles [52]. It was also found that 66.2% of the sub-basins are of orders 1 and 2 (Table 2). Overall, the number of streams tends to decrease as the order increases, as does the number of sub-basins corresponding to each order. On the other hand, it was shown that the area of the sub-basins of order 5 was greater than those of order 1, despite the fact that the amount is much smaller. Consequently, it can be said that the stream order is directly proportional to the drained area under normal conditions, and thus to the flow rate, as previously described.

**Table 2.** Stream order of the Sinú river basin.

| Order | Stream Number | Number of Sub-Basins | Sub Sub-Basins (km <sup>2</sup> ) | Total Streams Length (km) | Average Stream Length (km) | Stream Length Ratio ( $R_l$ ) | Bifurcation Ratio ( $R_b$ ) |
|-------|---------------|----------------------|-----------------------------------|---------------------------|----------------------------|-------------------------------|-----------------------------|
| 1     | 166           | 22                   | 4290.49                           | 680.47                    | 4.10                       | 8.30                          | 7.22                        |
| 2     | 23            | 21                   | 4952.43                           | 782.76                    | 34.03                      | 1.05                          | 3.83                        |
| 3     | 6             | 8                    | 1183.88                           | 214.21                    | 35.7                       | 1.19                          | 2.00                        |
| 4     | 3             | 6                    | 832.1                             | 127.39                    | 42.46                      | 11.41                         | 3                           |
| 5     | 1<br>199      | 8<br>65              | 2712.76<br>13,971.7               | 484.66<br>2289.50         | 484.66                     | 5.50                          | 7.60                        |

Additionally, during the analysis it was found that the number of streams progressively decreased as the order increased (Table 2). Out of the total of 199 streams found in the basin, 83% (166) are of order 1, 11.5% (23) of order 2, 3% (6) are of order 3, 1.5% (3) of order 4, and the main current is order of 5.

The values of the total and average length of the channels for each order can be seen in Table 2, where it is evident that 54.4% (1245.5 km) of the streams in the basin are of orders 1 and 2. These results corroborate the law of Horton stream lengths [4], which states that: “the average stream lengths of each order in a drainage basin tend to approximate a direct geometric series in which the first term is the average length of streams of order 1”. This is because, when making the graph of the logarithm of the length means against the stream order (Figure 6), it is evident that the points tend to a straight line. In this manner, it can be stated that the drainage network of the Sinú river complies with what was established by Horton [4] in terms of the behavior of the quantity and average length of the streams of a certain order. This implies that in the study area, the streams of order 1, having a lower mean length than the others, prevail in the areas where the steepest slopes are found.

**Figure 6.** Horton’s law of stream length for Sinú river basin, Colombia.

The obtained values of  $R_l$  for the different stream orders in the study area can be seen in Table 2, where it is evident that they range from 1.05 to 11.41.

In addition, the highest  $R_b$  was 7.22 and was calculated between the first and second order streams (Table 2), indicating that the longest overland flow lengths and the highest flows occur in these channels. The weighted average of the bifurcation ratio  $R_{bm}$  allows a representative value to be determined for the entire study area, estimated by multiplying the bifurcation ratio for each successive pair of orders times the total number of flows

involved in the ratio and taking the mean of the sum of these values [20,21]. For the study area, the  $R_{bm}$  was 7.6, which is higher than the arithmetic average of the estimated  $R_b$  (4.01).

When estimating drainage density from the results of the terrain modeling, it was found that it ranges between 0.06 km/km<sup>2</sup> and 0.24 km/km<sup>2</sup> for the 65 sub-basins obtained, 0.16 km/km<sup>2</sup> being the value obtained when analyzing the basin as a single area.

That said, it is necessary to clarify that this parameter is sensitive to the used threshold, so its interpretation must be carried out considering the other basin morphometric features. As a result, it was decided to corroborate the values obtained for these parameters using the cartographic plates at a scale of 1: 25,000 from the IGAC [44]. In this sense, when estimating the drainage density of the Sinú river basin from the available cartography, it was found that Dd is 1.59 km/km<sup>2</sup>, i.e., the drainage density obtained through modeling is not consistent with the one from the cartography. This is due, as explained above, to the resolution of the DEM and the threshold used in the analysis, since these parameters are sensitive to scale, as mentioned by Londoño [53] in his research. Even though these values are higher than those obtained from the terrain modeling, according to what is mentioned by the CVS [30], it can be affirmed that the Sinú river basin shows a low drainage density for the magnitudes of flows found.

On the other hand, the  $L_{OF}$  provides information on the hydrological response and the basin topography. In the case of the study area, it was found that the  $L_{OF}$  has a value of 0.31 km (Table 3), while in the sub-basins it ranges between 0.14 km and 29 km, reflecting that there is a significant variation in the basin relief features such as elevations and slope (See Figures 7 and 8). Correspondingly, Figure 7 shows that the upper Sinú is characterized by elevations higher than 150 masl, classified as hillside, mountain range, and ridges, whereas in the lower and middle Sinú there is a predominance of elevations below 350 masl (lowland and hillside).

**Table 3.** Morphometric Parameters: Drainage network of Sinú River Watershed.

| Morphometric Parameter  | Results |
|---|---------|
| <b>Drainage network</b>   |         |
| Stream order  | 5.00    |
| Stream length ( $L$ ) in km                                     | 243.80  |
| Stream length ( $L_u$ )   | -       |
| Number of streams ( $N_u$ )                                     | -       |
| Stream axial length ( $L_a$ ) in km                             | 184.90  |
| Drainage density ( $D_d$ ) km/km <sup>2</sup>                   | 1.59    |
| Length of overland flow ( $L_{OF}$ ) in km                      | 0.31    |
| Constant of channel maintenance ( $C_m$ ) in km/km <sup>2</sup> | 0.63    |
| Stream frequency ( $F$ ) in channels/km <sup>2</sup>            | 1.82    |
| Average stream length ( $L_m$ ) in km                           | -       |
| Sinuosity ( $S$ )   | 1.32    |
| Bifurcation ratio ( $R_b$ )                                     | -       |
| Mean bifurcation ratio ( $R_{bm}$ )                             | 2.88    |
| Stream length ratio ( $R_l$ )                                   | -       |

The  $C_m$  depends on factors such as relief and lithology, which in the case of the study area ranges between 0.28 km/km<sup>2</sup> and 59 km/km<sup>2</sup> for the sub-basins, with prevailing values of less than 10 km/km<sup>2</sup>. The value obtained for the entire basin (total area) was 0.63 km/km<sup>2</sup>, which is below the average of the values obtained in the sub-basins. This confirms what was previously described, where it was established that there are areas in the basin more susceptible to erosion due to the high slopes.

When analyzing the stream frequency ( $F$ ) for the case under study, it was found that in the sub-basins of the Sinú river, values lower than 4 channels/km<sup>2</sup> prevail, with the arithmetic mean being 1.68 channels/km<sup>2</sup> and the value for the entire basin being 1.82 channels/km<sup>2</sup> (Table 3).

In the study area, it was found that the stream sinuosity of the Sinú river is 1.32, indicating that the stream is sinuous according to what was found by Ahmed [52]. Additionally, it was observed that 87.7% (57) of the main streams of the sub-basins obtained in the modeling have a sinuosity lower than 1.25, indicating that their alignments tend to be straight and that the runoff speed is relatively high compared to the rest of the sub-basins.

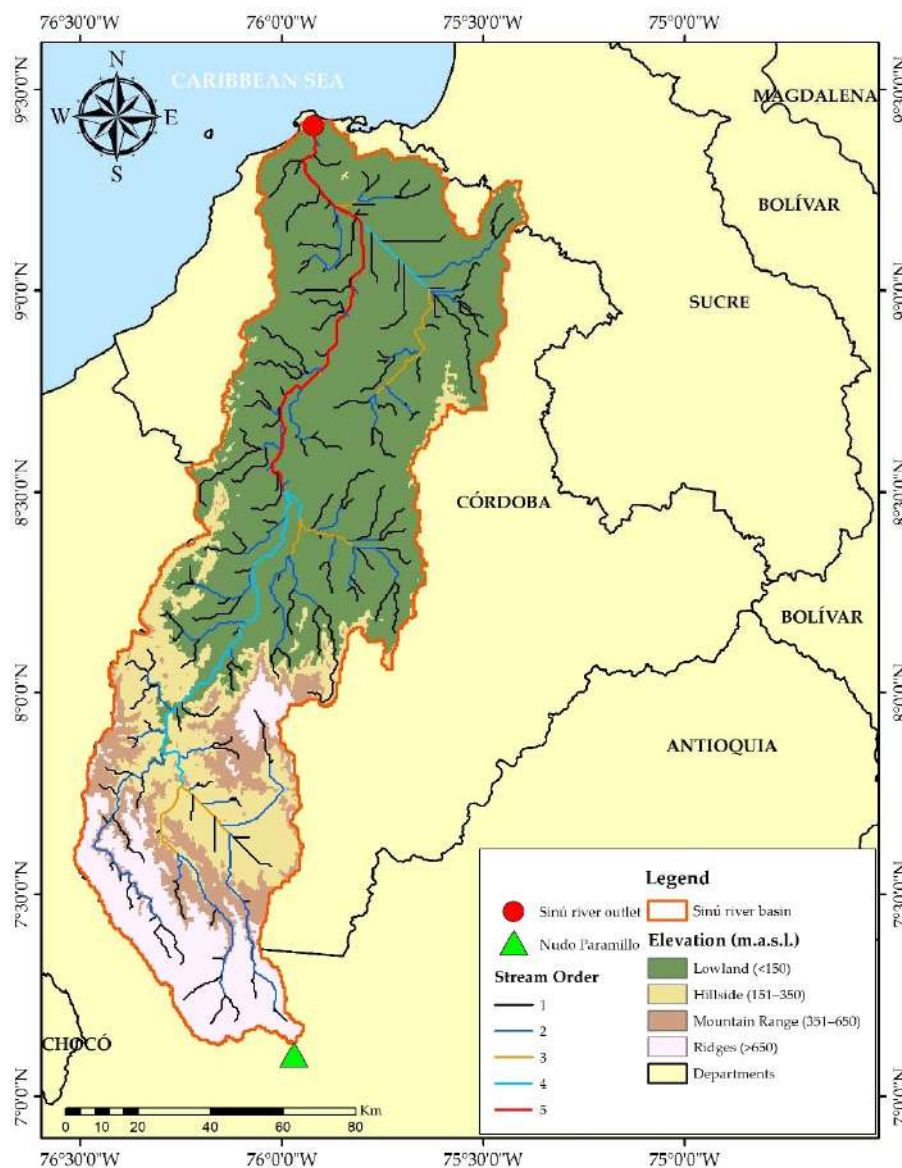
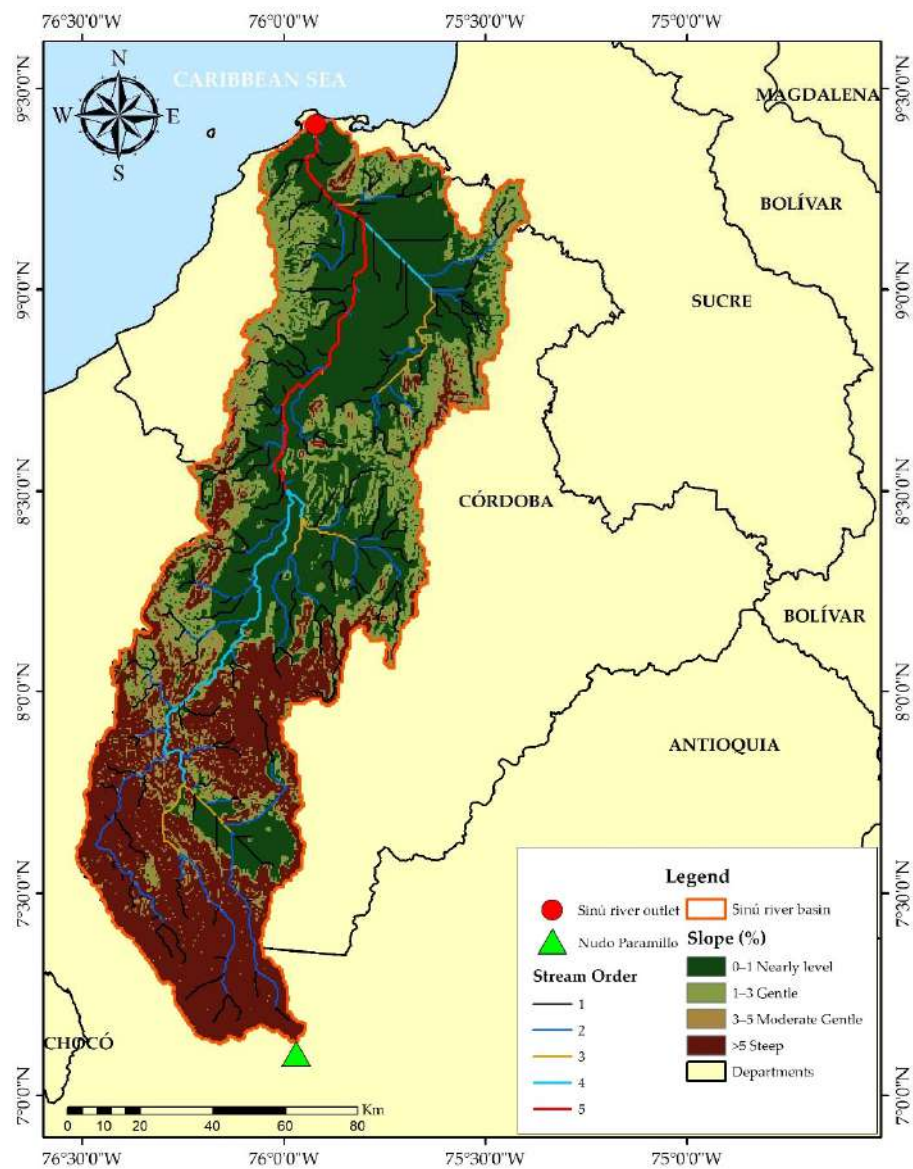


Figure 7. Elevation map of the Sinú river basin, Colombia.



**Figure 8.** Slope distribution map of the Sinú river basin, Colombia.

#### 4.2. Basin Geometry

The calculated geometry parameters can be found in Table 4. In the case of this research, the  $F_f$  for the sub-basins ranged between 0.186 and 0.721, with 90.8% (59 sub-basins) being less than 0.57, while the entire basin has an  $F_f$  of 0.22, indicating that it has an elongated shape. Similarly, the  $R_c$  values obtained for the 65 sub-basins vary between 0.17 and 0.49, 0.17 being for the complete basin. Additionally, the study area has an  $R_c$  of 0.53, making it an elongated basin, while the sub-basins have values that oscillate between 0.49 and 0.96, where 81.5% (53 sub-basins) show an  $R_c$  of less than 0.79. The estimated value of  $K_c$  was 2.43, while in the sub-basins values were between 1.42 and 2.40. This way, it becomes evident that all the sub-basins have elongated shapes according to this parameter.



**Table 4.** Morphometric Parameters: Geometry of Sinú River Watershed.

| Morphometric Parameter                  | Results   |
|---|-----------|
| <b>Basin geometry</b>                   |           |
| Basin area ( $A_d$ ) in km <sup>2</sup> | 13,971.70 |
| Basin perimeter ( $P$ ) in km           | 1025.90   |
| Basin length ( $L_c$ ) in km            | 252.40    |
| Form factor ( $F_f$ )                   | 0.22      |
| Circularity ratio ( $R_c$ )             | 0.17      |
| Elongation ratio ( $R_e$ )              | 0.53      |
| Compactness coefficient ( $K_c$ )       | 2.43      |

#### 4.3. Basin Relief

The relief of the basin was analyzed through GIS, the basin average slope was estimated as the average of the values of the slope grid generated from the elevation map (Figure 7), obtaining a value of 5.5%. Similarly, the map of the slopes of the study area was obtained (Figure 8) in which it can be observed that the upper Sinú basin is where the highest slopes occur, which may be responsible for the highest flows, while in the lower and middle Sinú basins, they decrease, forming extensive plains.

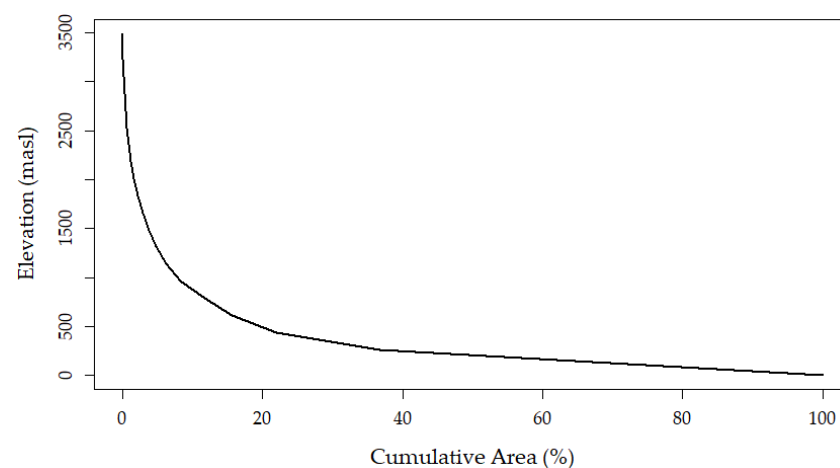
Additionally,  $H$  is 3493 m above sea level and 0 m above sea level, respectively, so the relief of the basin is 3493 m (Table 5).

**Table 5.** Morphometric Parameters: Relief of Sinú River Watershed.

| Morphometric Parameter                     | Results |
|--|---------|
| <b>Basin relief</b>                        |         |
| Minimum basin height ( $H_{min}$ ) in masl | 3493    |
| Maximum basin height ( $H_{max}$ ) in masl | 0.00    |
| Mean basin slope ( $S_c$ ) in percentage   | 5.50    |
| Basin relief ( $H$ )                       | 3493    |
| Relief ratio ( $F_H$ )                     | 13.83   |

Similarly, Schumm [20] defined the relief factor ( $F_H$ ) as the ratio between the basin relief ( $H$ ) and its maximum length ( $L_c$ ). For the Sinú river basin, the estimated  $F_H$  was 13.83.

On the other hand, Figure 9 shows the hypsometric curve of the Sinú river basin, where the highest slopes occur at the maximum elevations, which translates into areas with steep and mountainous terrain. Similarly, it is evident that most of the terrain has gentle slopes and uniform heights, which, according to Richardson et al. [54], suggests the existence of plains within the basin.

**Figure 9.** Hypsometric curve of the Sinú river basin.

#### 4.4. Rainwater Harvesting Potential Index (RWHPI)

The obtained results for RWHPI were classified using the quantile technique. Thus, for the Sinú river basin, the potential rainwater harvesting zones are classified as (a) 'Very high' (RWHPI = 0.266–0.334), (b) 'High' (RWHPI = 0.265–0.259), (c) 'Moderate' (RWHPI = 0.250–0.258), and (d) 'Poor' (RWHPI = 0.189–0.249). Figure 10 shows the rainwater harvesting potential zones for the Sinú river basin.

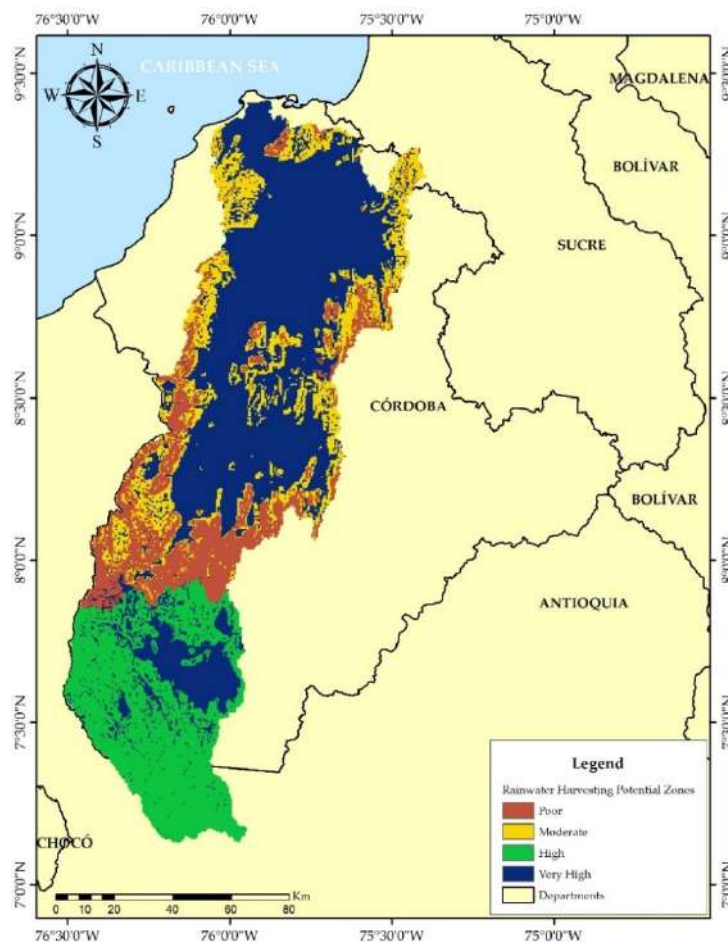


Figure 10. Map of the Sinú River Basin depicting Rainwater Harvesting Potential Zones.

## 5. Discussion

### 5.1. Drainage Network

The results of the morphometric parameters of the drainage network allow us to understand the basin hydrological behavior. First, the number of channels of order  $u$  is relevant, given that, if two basins are compared, the number of channels is an important factor, because if there is a greater number of streams, it can be inferred that there is better drainage and thus less permeability and infiltration, as mentioned by Rai et al. [6].

In accordance with the research of Ahmed et al. [55] and Rai et al. [6], the obtained results from the analysis of drainage density indicate that it is a basin with poor drainage where surface runoff cannot be quickly evacuated and, therefore, it is highly susceptible to floods. This parameter is also related to aspects such as soil erosion and runoff, since flow is directly proportional to drainage density, which translates into rapid runoff that implies, in turn, a flow of greater magnitude. Furthermore, it has an inverse relationship with infiltration, since high infiltration tends to inhibit the development of longer drains, i.e., as mentioned by Strahler [21], Bhagwat et al. [47], and Gajbhiye et al. [10,13], the lowest drainage densities correspond to regions with permeable soil types, dense vegetation, and

low relief, while high drainage density prevails in regions with impermeable soils, sparse vegetation, and high relief.

Figure 11 shows the histogram built to analyze the drainage density behavior in the 65 sub-basins, finding that values less than  $1.6 \text{ km/km}^2$  predominate in the basin and that there are some sub-basins where the value of  $D_d$  is less than unity. These results indicate that there are areas within the basin, such as the middle and lower Sinú areas, characterized by permeable soils and floodplains, while the upper Sinú is a region where impermeable soils with scarce vegetation that favor erosive processes and rapid flows prevail. It should be noted that for the variation analysis of the morphometric parameters in the sub-basins of the study area, histograms were constructed for each.

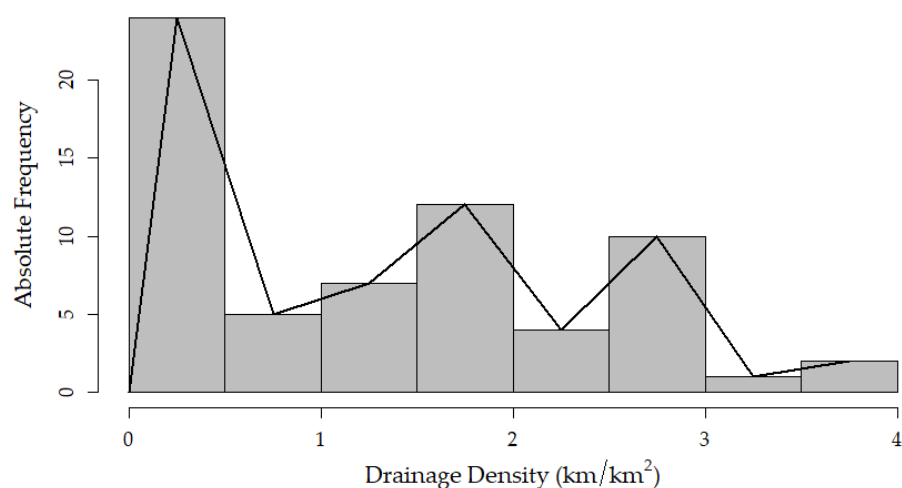


**Figure 11.** Histogram for drainage density analysis in the Sinú river basin.

Similarly, according to the research of Gayen et al. [56], Abboud and Nofal [57], Rai et al. [23], and Ameri et al. [7], it can be stated that the areas where the length of the overland flow is greater, are more susceptible to erosion and also reflect the presence of steep slopes. While the regions where this parameter is lower, are areas where less rain is required to generate significant flows. With these results, the heterogeneity of the geomorphological features of the basin is confirmed and it is inferred that the areas with the greatest susceptibility to erosion correspond to the upper Sinú, while the middle and lower Sinú are susceptible to flooding due to the fact that less precipitation is required to generate surface runoff.

Likewise, the variation in the results of the constant of channel maintenance corroborates the previous statement, due to the fact that values that exceed the mean value allow us to infer that a larger area is required to produce surface runoff towards the drainage network, which, as reported by Bhagwat et al. [47], favors losses by evaporation and infiltration. Otherwise, it happens with values below the average, since these favor rapid runoff and minimize the likelihood of these losses to occur. From the above, it follows that the high values correspond to the lower and middle Sinú where the terrain is relatively flat, while the low values are linked to the upper Sinú where slopes are higher.

According to what was found by Ozdemir and Bird [58] and Ameri et al. [7], the stream frequency is related to relief, vegetation cover, soil infiltration capacity, and susceptibility to erosion of a basin. Thus, it can be inferred that the areas where the highest drainage frequencies occur imply the presence of rocky surfaces, with low infiltration capacity and susceptibility to erosion. In the case of the Sinú river basin, values of  $F$  less than  $1.68 \text{ channels/km}^2$  predominate in the middle and lower Sinú regions, where the low slope and the uniformity of the elevations inhibit the generation of water currents, while the upper Sinú shows higher values of  $F$  due to the high slopes, coinciding with what was found when analyzing  $D_d$ .

Furthermore, the bifurcation ratio between the first and second order streams is much higher than those obtained for the rest of the orders, so it is indicative that in the areas where streams of these orders predominate, runoff is faster than in the rest of the basin, and thus, said areas are more susceptible to flooding during precipitation events, as mentioned by Hajam et al. [59]. Additionally, according to the research by Magesh et al. [60],  $R_{bm}$  values range between 3 and 5 for basins where the influence of the geological structure on the drainage network is negligible, so it is inferred that the characteristics of the drainage network of the Sinú river basin are strictly linked to geology and relief. Similarly, as reported by Arulbalaji and Gurugnanam [61],  $R_b$  variation, which in this case ranges from 2 to 7.22, indicates that there is geological heterogeneity in the basin, so that the lowest  $R_b$  values indicate high permeability while higher  $R_b$  imply low permeability.

Moreover, there was a significant variation in the values obtained for length ratio, which, according to Singh et al. [59], is indicative of the fact that there is an important change in the hydrological characteristics of the underlying rock surfaces over the areas of consecutive flow orders. In other words, the behavior of the RI indicates that there is geological heterogeneity in the basin and also, according to Bali et al. [62], that there are considerable differences in the topography and slope of the different sub-basins in the study area.

It can be stated that the obtained results for the parameters of the drainage network are consistent with the available information for the study area. The estimated parameters for the middle and lower Sinu indicate that these are areas characterized by low relief, slope, and susceptibility to floods such as the one occurred in 2010 [37] in accordance with the topography, given that, as mentioned in the study area description, lowland landscapes prevail in the region. Moreover, the prevalence of alluvial deposits (Q-al) confirms the erosion and sedimentation processes inferred from the estimated parameters, since these deposits are the result of erosion and deposition of materials associated with the dynamics of rivers, in times of both high flow and dry periods, and which are typical of meandering rivers such as the Sinú river [63].

## 5.2. Basin Geometry

The geometric parameters of the basin show that it has an elongated shape. In the investigations of Javed et al. [64], Iqbal et al. [1], Patel et al. [65], and Nanda et al. [66], it is established that the basins with a high  $F_f$  (circular) have a maximum flow of greater magnitude and shorter duration, while the basins with a low  $F_f$  (elongated) have a maximum flow of lesser magnitude with a longer duration. This means that there is an inversely proportional relationship between concentration time and  $F_f$ . The obtained results for this parameter indicate that the sub-basins are characterized by having elongated shapes, and thus, high concentration times compared to circular basins that have the same area. Nonetheless, the variation in the obtained values implies that there are areas within the basin that are more susceptible to flooding, such as the middle and lower Sinú basins.

As for the obtained results for the circular ratio, it is established that the basin, in addition to having an elongated shape, shows variation in the  $R_c$  values, which, considering that it is influenced by multiple characteristics such as length and frequency of the channels, geology, climate, and slope, reflects the heterogeneity of the physical features of the area of study, as mentioned by Ameri et al. [7].

The elongation ratio allows to study a basin hydrological response, since for a given precipitation, the less elongated basins will have a higher peak discharge and higher flow velocities [67]. Consequently, according to the results of Magesh [60], the results obtained indicate the presence of steep slopes in the study area, as observed in the upper Sinú area (Figure 8).

Additionally, considering that the regions with circular shapes require less time to produce a maximum flow, and that low values of compactness coefficient imply greater susceptibility to erosion, the variation in the results confirms that there is an important variability in the relief of the study area [7,64].

### 5.3. Basin Relief

According to Reddy et al. [68] and Sreedevi et al. [50], high values of  $H$ , such as the one obtained, indicate that there are conditions of low infiltration and high surface runoff in the Sinú river basin. Additionally, the obtained results for relief factor reflects the presence of steep slopes and consequently, the high intensity of erosion processes that occur on the slopes and the sediment load downstream according to the work of Thomas et al. [69].

The results shown in the slope maps allows us to infer that the areas where the slope is low is where the mirrors or surface water bodies of the basin are located (lower and middle Sinú), while the highest percentage of the flow of the main currents comes from the southern area where the elevations and slopes are higher, favoring high drainage density and channel frequency [65,68].

Similarly, the hypsometric curve reflects the geomorphology of the area, with the upper Sinú region being the area characterized by the presence of steep mountains and the middle and lower Sinú, the areas of plains. According to Strahler [21,70], through features such as the area under the hypsometric curve, slope, inflection point, and sinuosity, information about the geology of the basin can be inferred, given that we generally have the same family of curves for a specific geological and climatic combination. In the case of the Sinú river basin, it is inferred that having an upwardly concave hypsometric curve, active fluvial and alluvial sedimentary processes prevail, the reason for which the material has been eroded and deposited in the lower parts of the basin. Moreover, these types of curves indicate that the basin area is concentrated in the lower parts, which implies the presence of deep boxed valleys characteristic of foothills and savannahs.

### 5.4. Rainwater Harvesting Potential Zones

According to the analysis conducted, more than 70% of the basin area has characteristics suitable for rainwater harvesting. Particularly, it was identified that the areas with a 'very high' RWHPI correspond mainly to the middle and lower Sinú regions. Most of the upper Sinú is characterized by a 'High' RWHPI; however, it is also evident that most of the zones with 'Poor' RWHPI are concentrated in the upper Sinú, specifically in the region close to the middle Sinú. On the other hand, the zones with 'moderate' RWHPI are scattered in small patches throughout the middle and lower Sinú. Finally, it is important to note that the areas with a 'very high' RWHPI coincide with the presence of water bodies such as reservoirs and swamps.

## 6. Conclusions

The morphometric analysis carried out from the terrain modeling in the Sinú river basin through GIS, the existing cartography review, and the estimation of physiographic parameters made it possible to establish the following conclusions:

The obtained results for morphometric parameters, such as hypsometric curve of the basin,  $D_d$ ,  $F$ , stream order, and  $L_{OF}$  corroborated that the lower and middle Sinu sub-basins are susceptible to floods as evidenced by the flood events that have historically occurred in the study area. Concomitantly, the results indicate that the upper Sinú sub-basin is susceptible to erosive processes, which was confirmed by the review of the available information on the geology and geomorphology of the study area, establishing that the basin is framed within two large geo-structures: the mountain range or Cordillera (upper Sinú) and the sedimentation mega-basin (middle and lower Sinú). Thus, it is established that the prevalence of alluvial deposits in the basin is due to the material resulting from erosive processes in the upper Sinú that ends up being transported to the rest of the basin. Therefore, the results validate the basin geological heterogeneity.

The results allow us to affirm that the study area shows favorable characteristics for implementing water catchment techniques that contribute to the integrated management of the basin's water resources. However, so far, adequate management has not been carried out, leaving all this water to be lost when it reaches the ocean, even though there are problems in most of the lower and middle Sinú basins, especially during the dry season,

where dead animals and the lack of water availability for human consumption are evident in some sectors. Considering the characteristics of the study area, techniques such as furrows and ridges built along contour lines and dams would be strategies that would make it possible to take advantage of and store water resources during the winter season to be used during the dry season. From the review of the results and the literature, it can be inferred that, under normal conditions, there is a directly proportional relationship between drainage order and flow, since stream order is directly proportional to watershed size, channel dimensions, and stream flow. Nonetheless, sometimes smaller areas have greater flow due to rainfall behavior or other factors. Runoff is a complex variable that depends on multiple conditions. In the specific case of the Sinú river basin, it was possible to establish that, due to flow regulation by the Urrá hydroelectric plant (upper Sinú), flows remain stable throughout the basin.

Finally, these findings will help for the further modeling of an integrated watershed for sustainable hydrological and hydrograph models that, besides, will help understand the relationship between hydrological variables and geomorphological parameters as guidance and decision-making instruments for the competent authorities to establish actions for the sustainable development of the watershed, flood control, water supply planning, water budgeting, and disaster mitigation within the Sinú river basin.

**Author Contributions:** Conceptualization, Juan Pablo Medrano-Barboza, Alvaro Alberto López-Lambraño, Alvaro López-Ramos and Luisa Martínez-Acosta; methodology, Juan Pablo Medrano-Barboza, Alvaro Alberto López-Lambraño, John Freddy Remolina López and Luisa Martínez-Acosta; software, Juan Pablo Medrano-Barboza and Guillermo J. Acuña; validation, Juan Pablo Medrano-Barboza, Alvaro Alberto López-Lambraño, Alvaro López-Ramos and Luisa Martínez-Acosta; formal analysis, Juan Pablo Medrano-Barboza, Alvaro Alberto López-Lambraño, Alvaro López-Ramos, John Freddy Remolina López, Guillermo J. Acuña and Luisa Martínez-Acosta; investigation, Juan Pablo Medrano-Barboza, Alvaro Alberto López-Lambraño, Alvaro López-Ramos, John Freddy Remolina López, Guillermo J. Acuña and Luisa Martínez-Acosta; writing—original draft preparation, Juan Pablo Medrano-Barboza, Alvaro Alberto López-Lambraño, Alvaro López-Ramos, John Freddy Remolina López, Guillermo J. Acuña and Luisa Martínez-Acosta; writing—review and editing, Juan Pablo Medrano-Barboza, Alvaro Alberto López-Lambraño and Luisa Martínez-Acosta. All authors have read and agreed to the published version of the manuscript.

**Funding:** This research was funded by Hidrus S.A. de C.V., Grupo Hidrus S.A.S., Universidad Pontificia Bolivariana Seccional Montería, grant number 267-07/22-G012, and Universidad Autónoma de Baja California (<https://ror.org/05xwcq167>) and the APC was funded by Universidad Pontificia Bolivariana (<https://ror.org/02dxm8k93>).

**Institutional Review Board Statement:** Not applicable.

**Informed Consent Statement:** Not applicable.

**Data Availability Statement:** The data presented in this study are openly available in the following sources: (a) The digital elevation model used is freely available on the U.S. Geological Survey website [39]; (b) The 1:25,000 scale cartographic plates of the Sinú river basin are freely available on the Agustín Codazzi Geographical Institute website [44].

**Conflicts of Interest:** The authors declare no conflict of interest.

## References

1. Iqbal, M.; Sajjad, H.; Bhat, F.A. Morphometric Analysis of Shaliganga Sub Catchment, Kashmir Valley, India Using Geographical Information System. *Int. J. Eng. Trends Technol.* **2013**, *4*, 10–21.
2. Sujatha, E.R.; Selvakumar, R.; Rajasimman, B. Watershed Prioritization of Palar Sub-Watershed Based on the Morphometric and Land Use Analysis. *J. Mt. Sci.* **2014**, *11*, 906–916. [[CrossRef](#)]
3. Chitra, C.; Alaguraja, P.; Ganeshkumari, K.; Yuvaraj, D.; Manivel, M. Watershed Characteristics of Kundah Sub Basin Using Remote Sensing and GIS Techniques. *Int. J. Geomat. Geosci.* **2011**, *2*, 311–335.
4. Horton, R.E. Erosional Development of Streams and Their Drainage Basins, Hydrophyical Approach to Quantitative Morphology. *Bull. Geol. Soc. Am.* **1945**, *40*, 275–370. [[CrossRef](#)]

5. Nneka, C.; Philip, A.; Nnadozie, O.P.; Ayogu, O. Morphometric Analysis and the Validity of Hortonian Postulations in Anambra Drainage Basin, Nigeria. *Spat. Inf. Res.* **2019**, *27*, 505–520. [[CrossRef](#)]
6. Rai, P.K.; Mishra, V.N.; Mohan, K. A Study of Morphometric Evaluation of the Son Basin, India Using Geospatial Approach. *Remote Sens. Appl. Soc. Environ.* **2017**, *7*, 9–20. [[CrossRef](#)]
7. Ameri, A.A.; Pourghasemi, H.R.; Cerda, A. Erodibility Prioritization of Sub-Watersheds Using Morphometric Parameters Analysis and Its Mapping: A Comparison among TOPSIS, VIKOR, SAW, and CF Multi-Criteria Decision Making Models. *Sci. Total Environ.* **2018**, *613–614*, 1385–1400. [[CrossRef](#)]
8. Rai, P.K.; Singh, P.; Mishra, V.N.; Singh, A.; Sajan, B.; Shahi, A.P. Geospatial Approach for Quantitative Drainage Morphometric Analysis of Varuna River Basin, India. *J. Landsc. Ecol.* **2019**, *12*, 1–25. [[CrossRef](#)]
9. Adnan, M.S.G.; Dewan, A.; Zannat, K.E.; Abdullah, A.Y.M. The Use of Watershed Geomorphic Data in Flash Flood Susceptibility Zoning: A Case Study of the Karnaphuli and Sangu River Basins of Bangladesh. *Nat. Hazards* **2019**, *99*, 425–428. [[CrossRef](#)]
10. Gajbhiye, S.; Mishra, S.K.; Pandey, A. Prioritizing Erosion-Prone Area through Morphometric Analysis: An RS and GIS Perspective. *Appl. Water Sci.* **2014**, *4*, 51–61. [[CrossRef](#)]
11. Malik, A.; Kumar, A.; Kandpal, H. Morphometric Analysis and Prioritization of Sub-Watersheds in a Hilly Watershed Using Weighted Sum Approach. *Arab. J. Geosci.* **2019**, *12*, 118. [[CrossRef](#)]
12. Nitheshnirmal, S.; Thilagaraj, P.; Rahaman, S.A.; Jegankumar, R. Erosion Risk Assessment through Morphometric Indices for Prioritisation of Arjuna Watershed Using ALOS-PALSAR DEM. *Model. Earth Syst. Environ.* **2019**, *5*, 907–924. [[CrossRef](#)]
13. Rahmati, O.; Samadi, M.; Shahabi, H.; Azareh, A.; Rafiei-Sardooi, E.; Alilou, H.; Melesse, A.M.; Pradhan, B.; Chapi, K.; Shirzadi, A. Geoscience Frontiers SWPT: An Automated GIS-Based Tool for Prioritization of Sub-Watersheds Based on Morphometric and Topo-Hydrological Factors. *Geosci. Front.* **2019**, *10*, 2167–2175. [[CrossRef](#)]
14. Singh, L.K.; Jha, M.K.; Chowdary, V.M. Multi-Criteria Analysis and GIS Modeling for Identifying Prospective Water Harvesting and Artificial Recharge Sites for Sustainable Water Supply. *J. Clean. Prod.* **2017**, *142*, 1436–1456. [[CrossRef](#)]
15. Ezzeldin, M.; Konstantinovich, S.E.; Igorevich, G.I. Determining the Suitability of Rainwater Harvesting for the Achievement of Sustainable Development Goals in Wadi Watir, Egypt Using GIS Techniques. *J. Environ. Manag.* **2022**, *313*, 114990. [[CrossRef](#)]
16. Jena, S.K.; Tiwari, K.N. Modeling Synthetic Unit Hydrograph Parameters with Geomorphologic Parameters of Watersheds. *J. Hydrol.* **2006**, *319*, 1–14. [[CrossRef](#)]
17. Viramontes-Olivas, O.A.; Escoboza-García, L.F.; Pinedo-Álvarez, C.; Pinedo-Álvarez, A.; Reyes-Gómez, V.M.; Román-Calleros, J.A.; Pérez-Márquez, A. Morfometría de La Cuenca Del Río San Pedro, Conchos, Chihuahua. *Tecnociencia* **2007**, *1*, 21–31.
18. Escalante, C.A.; Reyes, L. *Técnicas Estadísticas En Hidrología*; Facultad de Ingeniería, Universidad Autónoma de México: Mexico City, Mexico, 2002.
19. Horton, R.E. Drainage-Basin Characteristics. *Eos Trans. Am. Geophys. Union* **1932**, *13*, 350–361. [[CrossRef](#)]
20. Schumm, S. Evolution of Drainage Systems and Slopes in Badland at Peth Amboy, New Jersey. *Geol. Soc. Am. Bull.* **1956**, *67*, 597–646. [[CrossRef](#)]
21. Strahler, A.N. Quantitative Classification of Watershed Geomorphology. *Trans. Am. Geophys. Union* **1957**, *38*, 913–920. [[CrossRef](#)]
22. Shreve, R.L. Statistical Law of Stream Numbers. *J. Geol.* **1966**, *74*, 17–37. [[CrossRef](#)]
23. Rai, P.K.; Chaubey, P.K.; Mohan, K.; Singh, P. Geoinformatics for Assessing the Inferences of Quantitative Drainage Morphometry of the Narmada Basin in India. *Appl. Geomat.* **2017**, *9*, 167–189. [[CrossRef](#)]
24. Alqahtani, F.; Qaddah, A.A. GIS Digital Mapping of Flood Hazard in Jeddah-Makkah Region from Morphometric Analysis. *Arab. J. Geosci.* **2019**, *12*, 199. [[CrossRef](#)]
25. Mangan, P.; Haq, M.A.; Baral, P. Morphometric Analysis of Watershed Using Remote Sensing and GIS—A Case Study of Nanganji River Basin in Tamil Nadu, India. *Arab. J. Geosci.* **2019**, *12*, 202. [[CrossRef](#)]
26. Panda, B.; Venkatesh, M.; Kumar, B. A GIS-Based Approach in Drainage and Morphometric Analysis of Ken River Basin and Sub-Basins, Central India. *J. Geol. Soc. India* **2019**, *93*, 75–84. [[CrossRef](#)]
27. Prakash, K.; Rawat, D.; Singh, S.; Chaubey, K.; Kanhaiya, S.; Mohanty, T. Morphometric Analysis Using SRTM and GIS in Synergy with Depiction: A Case Study of the Karmanasa River Basin, North Central India. *Appl. Water Sci.* **2019**, *9*, 1–10. [[CrossRef](#)]
28. Shivhare, V.; Gupta, C.; Mallick, J.; Singh, C.K. Geospatial Modelling for Sub-Watershed Prioritization in Western Himalayan Basin Using Morphometric Parameters. *Nat. Hazards* **2022**, *110*, 545–561. [[CrossRef](#)]
29. Shrivatra, J.R.; Manjare, B.S.; Paunikar, S.K. A GIS-Based Assessment in Drainage Morphometry of WRJ-1 Watershed in Hard Rock Terrain of Narkhed Taluka, Maharashtra, Central India. *Remote Sens. Appl. Soc. Environ.* **2021**, *22*, 100467. [[CrossRef](#)]
30. Corporación Autónoma Regional de los Valles del Sinú y San Jorge (CVS). *Fases de Prospección y Formulación Del Plan de Ordenamiento y Manejo Integral de La Cuenca Hidrográfica Del Río Sinú (POMCA-RS)*; CVS: Montería, Colombia, 2006.
31. Valbuena, D.L. *Geomorfología y Condiciones Hidráulicas Del Sistema Fluvial Del Río Sinú. Integración Multiescalar. 1945–1999–2016*; Universidad Nacional de Colombia: Bogotá, Colombia, 2017.
32. Instituto Geográfico Agustín Codazzi (Ed.) *Estudio General de Suelos y Zonificación de Tierras, Departamento de Córdoba*, 1st ed.; Imprenta Nacional de Colombia: Bogotá, Colombia, 2009.
33. Remane, J. *Explanatory Note to the International Stratigraphic Chart*; International Union of Geological Sciences: Trondheim, Norway, 2000.

34. Gómez, J.; Nivia, Á.; Montes, N.E.; Almanza, M.F.; Alcárcel, F.A.; Madrid, C.A. Notas Explicativas: Mapa Geológico de Colombia. In *Compilando la Geología de Colombia: Una Visión a 2015*; Gómez, J., Almanza, M.F., Eds.; Servicio Geológico Colombiano: Bogotá, Colombia, 2015; Volume 33, pp. 9–33.
35. BID; CEPAL; DNP. *Valoración de Daños y Pérdidas. Ola Invernal En Colombia 2010–2011*; Misión BID—Cepal: Bogotá, Colombia, 2012; 240p.
36. IDEAM. *Estudio Nacional Del Agua 2018*; Instituto de Hidrología, Meteorología y Estudios Ambientales: Bogotá, Colombia, 2019; ISBN 9789585489127.
37. CVS. *Puntos Críticos Cuenca Sinú*; CVS: Montería, Colombia, 2019.
38. Felicísimo, A.M. *Modelos Digitales Del Terreno. Introducción y Aplicaciones En Las Ciencias Ambientales*; Pentalfa Ediciones: Oviedo, Spain, 1994.
39. U.S. Geological Survey (USGS). HydroSHEDS 15 Arc-Second DEMs for South America. Available online: <http://hydrosheds.cr.usgs.gov> (accessed on 28 May 2018).
40. Rineer, J.; Bruhn, M.; Miralles-Wilhelm, F. *Nota Técnica Base de Datos de Hidrología Analítica Para América Latina y El Caribe*; Banco Interamericano de Desarrollo (BID): Washington, DC, USA, 2014.
41. Jenson, K.; Domingue, O. Extracting Topographic Structure from Digital Elevation Data for Geographic Information System Analysis. *Photogramm. Eng. Remote Sens.* **1988**, *54*, 1593–1600.
42. Mueller, J.E. An Introduction to the Hydraulic and Topographic Sinuosity Indexes. *Ann. Assoc. Am. Geogr.* **1968**, *58*, 371–385. [[CrossRef](#)]
43. Martínez-Acosta, L.; López-Lambraño, A.A.; López-Ramos, A. Design Criteria for Planning the Agricultural Rainwater Harvesting Systems: A Review. *Appl. Sci.* **2019**, *9*, 5298. [[CrossRef](#)]
44. Instituto Geográfico Agustín Codazzi Datos Abiertos Cartografía y Geografía-Cartografía Base Escala 1:25,000. Available online: <https://geoportal.igac.gov.co/contenido/datos-abiertos-cartografia-y-geografia> (accessed on 27 May 2018).
45. Miller, V.C. *A Quantitative Geomorphologic Study of Drainage Basin Characteristics in the Clinch Mountain Area, Virginia and Tennessee*; Technical report; Columbia University: New York, NY, USA, 1953.
46. Magesh, N.S.; Jitheshlal, K.V.; Chandrasekar, N.; Jini, K.V. GIS Based Morphometric Evaluation of Chimmini and Mupily Watersheds, Parts of Western Ghats, Thrissur District, Kerala, India. *Earth Sci. Inform.* **2012**, *5*, 111–121. [[CrossRef](#)]
47. Bhagwat, T.N.; Shetty, A.; Hegde, V.S. Spatial Variation in Drainage Characteristics and Geomorphic Instantaneous Unit Hydrograph (GIUH); Implications for Watershed Management-A Case Study of the Varada River Basin, Northern Karnataka. *Catena* **2011**, *87*, 52–59. [[CrossRef](#)]
48. Pareta, K.; Pareta, U. Quantitative Morphometric Analysis of a Watershed of Yamuna Basin, India Using ASTER (DEM) Data and GIS. *Int. J. Geomat. Geosci.* **2011**, *2*, 248–269.
49. Chopra, R.; Dhiman, R.D.; Sharma, P.K. Morphometric Analysis of Sub-Watersheds in Gurdaspur District, Punjab Using Remote Sensing and GIS Techniques. *J. Indian Soc. Remote Sens.* **2005**, *33*, 531–539. [[CrossRef](#)]
50. Sreedevi, P.D.; Subrahmanyam, K.; Ahmed, S. The Significance of Morphometric Analysis for Obtaining Groundwater Potential Zones in a Structurally Controlled Terrain. *Environ. Geol.* **2005**, *47*, 412–420. [[CrossRef](#)]
51. Hajam, R.A.; Hamid, A.; Bhat, S. Application of Morphometric Analysis for Geo-Hydrological Studies Using Geo-Spatial Technology—A Case Study of Vishav Drainage Basin. *J. Waste Water Treat. Anal.* **2013**, *4*, 12. [[CrossRef](#)]
52. Ahmed, A.A.; Fawzi, A. Meandering and Bank Erosion of the River Nile and Its Environmental Impact on the Area between Sohag and El-Minia, Egypt. *Arab. J. Geosci.* **2011**, *4*, 1–11. [[CrossRef](#)]
53. Londoño Arango, C. *Cuencas Hidrográficas: Bases Conceptuales, Caracterización, Administración*; Universidad del Tolima: Ibagué, Colombia, 2001.
54. Richardson, J.C.; Hodgson, D.M.; Wilson, A.; Carrivick, J.L.; Lang, A. Testing the Applicability of Morphometric Characterisation in Discordant Catchments to Ancient Landscapes: A Case Study from Southern Africa. *Geomorphology* **2016**, *261*, 162–176. [[CrossRef](#)]
55. Ahmed, S.A.; Chandrashekarappa, K.N.; Raj, S.K.; Nischitha, V.; Kavitha, G. Evaluation of Morphometric Parameters Derived from ASTER and SRTM DEM—A Study on Bandihole Sub-Watershed Basin in Karnataka. *J. Indian Soc. Remote Sens.* **2010**, *38*, 227–238. [[CrossRef](#)]
56. Gayen, S.; Bhunia, G.S.; Shit, P.K. Morphometric Analysis of Kangshabati-Darkeswar Interfluves Area in West Bengal, India Using ASTER DEM and GIS Techniques. *J. Geol. Geosci.* **2013**, *2*, 1–10. [[CrossRef](#)]
57. Abboud, I.A.; Nofal, R.A. Morphometric Analysis of Wadi Khumal Basin, Western Coast of Saudi Arabia, Using Remote Sensing and GIS Techniques. *J. Afr. Earth Sci.* **2017**, *126*, 58–74. [[CrossRef](#)]
58. Ozdemir, H.; Bird, D. Evaluation of Morphometric Parameters of Drainage Networks Derived from Topographic Maps and DEM in Point of Floods. *Environ. Geol.* **2009**, *56*, 1405–1415. [[CrossRef](#)]
59. Singh, P.; Thakur, J.K.; Singh, U.C. Morphometric Analysis of Morar River Basin, Madhya Pradesh, India, Using Remote Sensing and GIS Techniques. *Environ. Earth Sci.* **2013**, *68*, 1967–1977. [[CrossRef](#)]
60. Magesh, N.S.; Jitheshlal, K.V.; Chandrasekar, N.; Jini, K.V. Geographical Information System-Based Morphometric Analysis of Bharathapuzha River Basin, Kerala, India. *Appl. Water Sci.* **2013**, *3*, 467–477. [[CrossRef](#)]
61. Arulbalaji, P.; Gurugnanam, B. Geospatial Tool-Based Morphometric Analysis Using SRTM Data in Sarabanga Watershed, Cauvery River, Salem District, Tamil Nadu, India. *Appl. Water Sci.* **2017**, *7*, 3875–3883. [[CrossRef](#)]



62. Bali, R.; Agarwal, K.K.; Ali, S.N.; Rastogi, S.K.; Krishna, K. Drainage Morphometry of Himalayan Glacio-Fluvial Basin, India: Hydrologic and Neotectonic Implications. *Environ. Earth Sci.* **2012**, *66*, 1163–1174. [[CrossRef](#)]
63. Servicio Geológico Colombiano; Universidad Nacional de Colombia. *Memoria Técnica Explicativa Del Mapa Geomorfológico Analítico Aplicado a La Zonificación de Amenaza Por Movimientos En Masa Escala 1:100.000 Plancha 89bis–Río Salquí, Departamento de Chocó*; Universidad Nacional de Colombia: Bogotá, Colombia, 2015.
64. Javed, A.; Yousuf, M.; Rizwan, K. Prioritization of Sub-Watersheds Based on Morphometric and Land Use Analysis Using Remote Sensing and GIS Techniques. *J. Indian Soc. Remote Sens.* **2009**, *37*, 261–274. [[CrossRef](#)]
65. Patel, D.P.; Gajjar, C.A.; Srivastava, P.K. Prioritization of Malesari Mini-Watersheds through Morphometric Analysis: A Remote Sensing and GIS Perspective. *Environ. Earth Sci.* **2013**, *69*, 2643–2656. [[CrossRef](#)]
66. Nanda, A.M.; Ahmed, P.; Kanth, T.A.; Hajam, R.A. Morphometric Analysis of Sandran Drainage Basin (J & K) Using Geo—Spatial Technology. *Earth Sci. India* **2014**, *7*, 55–66.
67. Bajabaa, S.; Masoud, M.; Al-Amri, N. Flash Flood Hazard Mapping Based on Quantitative Hydrology, Geomorphology and GIS Techniques (Case Study of Wadi Al Lith, Saudi Arabia). *Arab. J. Geosci.* **2014**, *7*, 2469–2481. [[CrossRef](#)]
68. Reddy, G.P.O.; Maji, A.K.; Gajbhiye, K.S. Drainage Morphometry and Its Influence on Landform Characteristics in a Basaltic Terrain, Central India—A Remote Sensing and GIS Approach. *Int. J. Appl. Earth Obs. Geoinf.* **2004**, *6*, 1–16. [[CrossRef](#)]
69. Thomas, J.; Joseph, S.; Thri vikramji, K.P.; Abe, G.; Kannan, N. Morphometrical Analysis of Two Tropical Mountain River Basins of Contrasting Environmental Settings, the Southern Western Ghats, India. *Environ. Earth Sci.* **2012**, *66*, 2353–2366. [[CrossRef](#)]
70. Strahler, A.N. Hypsometric (Area-Altitude) Analysis of Erosional Topography. *Geol. Soc. Am. Bull.* **1952**, *63*, 1117–1142. [[CrossRef](#)]